

Influence of p-doping on the temperature dependence of InAs/GaAs quantum dot excited state radiative lifetime

Edmund Harbord, S. Iwamoto, Y. Arakawa, P. Spencer, E. Clarke et al.

Citation: *Appl. Phys. Lett.* **101**, 183108 (2012); doi: 10.1063/1.4765349

View online: <http://dx.doi.org/10.1063/1.4765349>

View Table of Contents: <http://apl.aip.org/resource/1/APPLAB/v101/i18>

Published by the [American Institute of Physics](http://www.aip.org).

Related Articles

Electrical excitation and detection of magnetic dynamics with impedance matching

Appl. Phys. Lett. **101**, 182402 (2012)

Atomic-resolution study of polarity reversal in GaSb grown on Si by scanning transmission electron microscopy

J. Appl. Phys. **112**, 093101 (2012)

Dielectric strength, optical absorption, and deep ultraviolet detectors of hexagonal boron nitride epilayers

Appl. Phys. Lett. **101**, 171112 (2012)

Effective passivation of In_{0.2}Ga_{0.8}As by HfO₂ surpassing Al₂O₃ via in-situ atomic layer deposition

Appl. Phys. Lett. **101**, 172104 (2012)

Atomic structure and energy spectrum of Ga(As,P)/GaP heterostructures

J. Appl. Phys. **112**, 083713 (2012)

Additional information on *Appl. Phys. Lett.*

Journal Homepage: <http://apl.aip.org/>

Journal Information: http://apl.aip.org/about/about_the_journal

Top downloads: http://apl.aip.org/features/most_downloaded

Information for Authors: <http://apl.aip.org/authors>

ADVERTISEMENT



Goodfellow
metals • ceramics • polymers • composites
70,000 products
450 different materials
small quantities fast

www.goodfellowusa.com

Influence of p-doping on the temperature dependence of InAs/GaAs quantum dot excited state radiative lifetime

Edmund Harbord,^{1,a)} S. Iwamoto,^{1,2} Y. Arakawa,^{1,2} P. Spencer,³ E. Clarke,⁴ and R. Murray³

¹NanoQUINE, the University of Tokyo, 4-6-1, Komaba, Meguro-ku, Tokyo 153-8505, Japan

²Institute of Industrial Science, the University of Tokyo, 4-6-1, Komaba, Meguro-ku, Tokyo 153-8505, Japan

³EXSS, The Blackett Laboratory, Imperial College London, Prince Consort Road, London SW7 2AZ, United Kingdom

⁴EPSRC National Centre for III-V Technologies, University of Sheffield, Sheffield S1 3JD, United Kingdom

(Received 21 August 2012; accepted 18 October 2012; published online 2 November 2012)

The radiative lifetime of the excited state transition of undoped and p-doped InAs/GaAs quantum dots (QDs) is estimated from measurements of time-integrated and time-resolved luminescence from both ground and excited states. The radiative lifetime of the undoped QDs increases from 500 ps at 10 K to almost 3 ns at room temperature, consistent with a Boltzmann redistribution of holes over the available energy states. The rate of increase can be suppressed by a factor of ~ 2 by p-doping the QDs to maintain a hole population in the lowest confined dot states to high temperatures. © 2012 American Institute of Physics. [<http://dx.doi.org/10.1063/1.4765349>]

InAs/GaAs quantum dots (QDs) are nanostructures that offer quasi-particle confinement in three dimensions. This confinement leads to energetic separation of the electron and hole states, making QDs an ideal gain medium for semiconductor lasers. They promise reduced threshold currents and higher T_0 ,¹ due to the suppression of hole spreading over the available energy states at elevated temperature. The potential for lasing may be further enhanced by locally p-doping spatially close to the QDs: this introduces a permanent population of holes into the QDs, suppressing thermal spreading. Additionally, this can result in an increased modulation speed for QD lasers.^{2,3} Above threshold, the higher injection rates result in state filling, and dual state lasing from the ground state (GS) and first excited state (X1) has been reported.^{4,5} Below threshold and in non-lasing structures, photoluminescence lifetime measurements can be used to determine the luminescence lifetimes. The interpretation of these is complicated by the simultaneous presence of non-radiative processes involving defects, relaxation and carrier escape at elevated temperatures. Accordingly, measurements of the radiative lifetime of the X1 transition in undoped and p-doped QDs over a wide range of temperatures are important for understanding the physics of QD lasers.

First, let us review previous publications that provide a backdrop for the present work. Although there has been one report of a single exponential decay of the X1 transition,⁶ biexponential decays are the norm.^{7–11} For example, Mukai *et al.*⁸ analysed the biexponential decays assuming a single radiative lifetime for all confined levels and attributed the presence of a faster component to relaxation to lower levels. Surprisingly, this component *decreased* with increasing temperature. By contrast, Gurioli *et al.*¹⁰ reported a fast component of 250 ps at 10 K which *increased* to 400 ps by 300 K. The increase was attributed to thermalization between the ground and the excited states at temperatures above 120 K. Siegert *et al.*¹² compared the low temperature (80 K) PL decays of heavily p-doped (~ 330 holes/QD) and n-doped

samples and found that the excited state decays were four times shorter than that of the undoped reference sample. The radiative lifetimes were not determined. In this letter, we experimentally recover the intuitively expected dynamics of the excited state of quantum dots. We report time integrated and time resolved spectroscopy on a control sample A, which consists of a single layer of undoped QDs and sample B, which consists of a single layer of QDs p-doped at a level equivalent to 10 holes per QD. Using these data, together with a simple model, the radiative lifetime can be extracted over the temperature range of 12 K–300 K. We find that the radiative lifetime of the undoped sample increases to almost 3 ns by room temperature. This increase is suppressed by a factor of 2 by p-doping.

Careful sample design is extremely important when attempting comparisons of doped and undoped samples. The dot layer was grown between two $\text{Al}_{0.3}\text{Ga}_{0.7}\text{As}$ layers to maintain a constant excitation volume. In order to avoid segregation of the Be atoms, doping was confined to a region above the QD layer ($\text{Al}_{0.3}\text{Ga}_{0.7}\text{As}$ layers have a much lower Be solubility¹³). Further growth details can be found in Ref. 14. AFM measurements of uncapped samples indicates that these samples have a QD areal density of $2 \times 10^{10} \text{ cm}^{-2}$. Although the doping level corresponds to 10 holes/QD, the Be doping density is an order of magnitude below that for which non-radiative mechanisms in the bulk GaAs are enhanced.¹⁵

The samples are excited by 790 nm 2.4 ps pulses from a Ti:Al₂O₃ laser at temperatures from 12 K to 300 K. PL is collected and dispersed by a monochromator and detected either using an LN₂ cooled Ge photodiode with lock-in detection (for the time integrated measurements) or by passing a 1 meV band to a microchannel plate with an extended S1 response using time-correlated single photon counting.

Low temperature (12 K) PL spectra obtained from sample A (sample B) are shown in Figure 1(a) (Figure 1(d)) under low (black, dashed line) and high (red, solid line) power excitations. The narrow size dispersion of the QD population is reflected in the width of the PL spectrum (~ 30 meV) under low power excitation. This allows emission from the first

^{a)}Electronic mail: harbord@iis.u-tokyo.ac.jp.

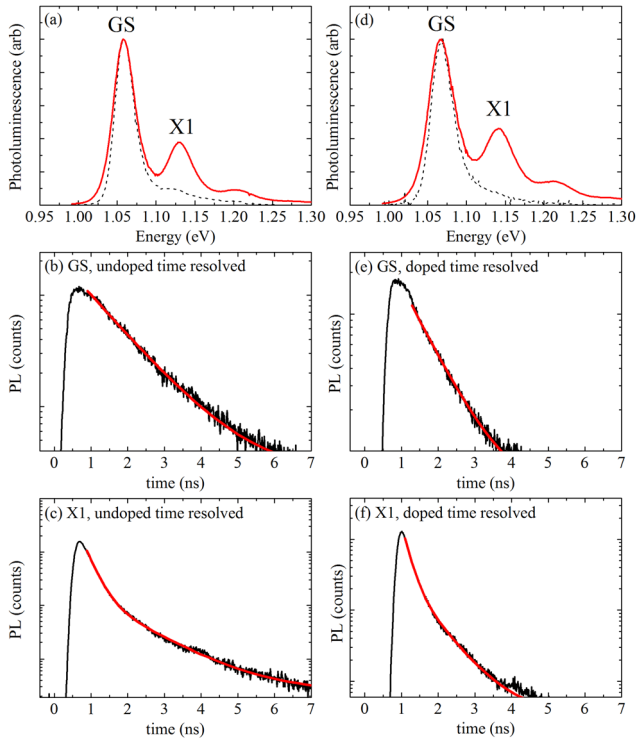


FIG. 1. (a) Time integrated PL spectra from sample A (undoped) at 12 K, normalized to the GS emission peak. The black dashed line shows the PL under low power excitation (0.5 W cm^{-2}); the red solid shows the PL under high power excitation (600 W cm^{-2}). The GS and X1 are labeled on the graph. Time-resolved PL from (b) GS and (c) X1 of sample A (undoped) at 12 K. The time resolved data are measured at the peak of the GS and X1, respectively, and the solid red lines show monoexponential (GS) and biexponential fits (X1). (d) Time integrated PL spectra from sample B (doped) at 12 K. The black dashed line shows the PL under low power excitation (0.5 W cm^{-2}); the red solid line shows the PL under high power excitation (600 W cm^{-2}). The GS and X1 are labeled on the graph. Time-resolved PL from (e) GS and (f) X1 of sample B (doped) at 12 K. The time resolved data are measured at the peak of the GS and X1, respectively, and the solid red lines show monoexponential (GS) and biexponential fits (X1).

excited state (X1) under high excitation to be clearly distinguished from the GS. The high energy shoulder of the distribution under low power excitation is associated with the presence of a subset of smaller QDs having higher energy ground states. By subtracting the normalized low power spectrum from the higher power spectrum, it is possible to remove

the contribution of these small, high energy QDs, leaving only the contribution from the X1 transition of the more numerous deeper QDs (PL_{X1}).¹¹

Time resolved data are shown in Figures 1(b), 1(c), 1(e), and 1(f) for the two samples. The GS luminescence from both samples exhibits monoexponential decay with a characteristic time τ_{GS} . The X1 luminescence exhibits a biexponential decay which we attribute to the two different QD populations: a faster component due to X1 of the deeper QDs, and a longer one due to the GS of the shallow QDs, which emit at the same wavelength. Details of the measurements that lead to this conclusion are contained in Ref. 11. By fitting to a biexponential decay, the shorter decay time $\tau_{\text{X1}}^{\text{lum}}$ associated with the pure X1 emission can be obtained.¹¹ These data are shown in Figures 2(a) and 2(c), for samples A and B, respectively.

In order to obtain the radiative lifetime of the X1 for both samples over the complete temperature range, a simple model of X1 luminescence is adapted from that used to describe the GS.¹⁴ The luminescence lifetime ($\tau_{\text{X1}}^{\text{lum}}$) of X1 has a radiative component ($\tau_{\text{X1}}^{\text{rad}}$) and a non-radiative component ($\tau_{\text{X1}}^{\text{nr}}$) which are related by

$$\frac{1}{\tau_{\text{X1}}^{\text{lum}}} = \frac{1}{\tau_{\text{X1}}^{\text{rad}}} + \frac{1}{\tau_{\text{X1}}^{\text{nr}}}. \quad (1)$$

The non-radiative component of the lifetime consists of two components: relaxation to the ground state followed by recombination there; and a temperature dependent escape mechanism followed by recombination elsewhere. At low temperature, we can assume that thermal carrier escape can be neglected and the last term reduced to accounting for the losses to the GS due to carrier relaxation only; relaxation to the ground state is much faster than radiative relaxation⁹ and given by

$$\frac{1}{\tau_{\text{X1}}^{\text{nr}}} \approx \frac{g_{\text{GS}}}{\tau_{\text{GS}}}, \quad (2)$$

where g_{GS} , τ_{GS} are the degeneracy and radiative lifetime of the GS, respectively. Subject to these two assumptions, at low temperature Eq. (1) can be written as

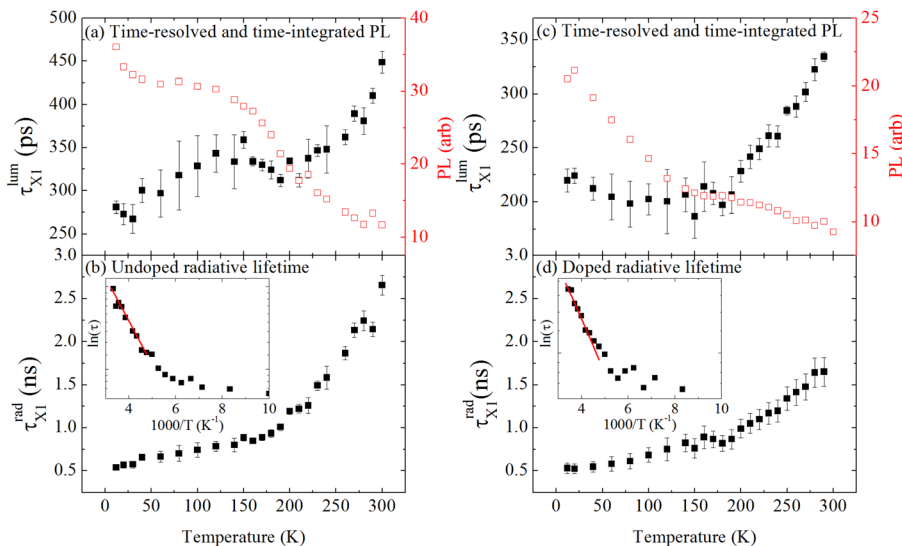


FIG. 2. (a) PL_{X1} (red, open squares) and τ_{X1} (black, closed squares) for the undoped sample. (b) The extracted radiative lifetime (τ_{X1}) for sample A (undoped), normalized to the low temperature value. Inset: this radiative lifetime (black squares) on an Arrhenius scale, together with fit (activation energy $\sim 43 \text{ meV}$). (c) PL_{X1} (red, open squares) and τ_{X1} (black, closed squares) for sample B (doped). (d) The extracted radiative lifetime for sample B (doped), normalized to the low temperature value. Inset: this radiative lifetime (black, closed squares) on an Arrhenius scale, together with fit (activation energy $\sim 36 \text{ meV}$).

TABLE I. Luminescence lifetimes for τ_{GS} , τ_{X1}^{lum} (from fitting to the PL decays), and τ_{X1}^{rad} (from Eq. (9)) for samples A and B measured at 12 K.

	τ_{GS} (ps)	τ_{X1}^{lum} (ps)	τ_{X1}^{rad} (ps)
A, undoped	1170 ± 12	280 ± 10	540 ± 20
B, p-doped	755 ± 30	220 ± 30	530 ± 20

$$\frac{1}{\tau_{X1}^{lum}} = \frac{1}{\tau_{X1}^{rad}} + \frac{g_{GS}}{\tau_{GS}}. \quad (3)$$

Carriers are photo-generated at a rate G , so the number of electrons in the QD excited state can be described by

$$\frac{dN}{dt} = G - \frac{N}{\tau_{X1}^{lum}}. \quad (4)$$

In the steady state, $N = G\tau_{X1}^{lum}$, so the PL from the excited state can be expressed as

$$PL_{X1} \propto \frac{N}{\tau_{X1}^{rad}} = G \frac{\tau_{X1}^{lum}}{\tau_{X1}^{rad}}. \quad (5)$$

Hence,

$$\tau_{X1}^{rad} \propto \frac{\tau_{X1}^{lum}}{PL_{X1}}. \quad (6)$$

At low temperature, the radiative lifetime τ_{X1}^{rad} may be calculated from Eq. (3) under the assumption that $g_{GS} = 2$.¹⁶ These lifetimes for both samples are shown in Table I. These values, together with Eq. (6), can then be used to estimate the radiative lifetime over the complete temperature range as shown in Figures 2(b) and 2(d) for the undoped (A) and doped (B) samples, respectively.

The X1 radiative lifetime of the undoped sample doubles in value from 500 ps at 12 K to 1 ns at 200 K. Above 200 K, this increase triples to reach 3 ns by room temperature. The inset Arrhenius plot of Figure 2(b) shows the activation energy of 43 ± 5 meV. The X1 radiative lifetime of the p-doped sample also increases with temperature, but more gradually; the increase is suppressed by a factor of almost 2. The inset Arrhenius plot of Figure 2(d) shows activation energy of 36 ± 5 meV.

We can qualitatively explain this behavior by considering the mechanism responsible for the increase of radiative lifetime with temperature. In bulk semiconductors,¹⁷ Boltzmann spreading over the close energy levels leads to recombination being forbidden by the selection rules, increasing the radiative lifetime; in low dimensional semiconductor nanostructures, the quantum confinement effect leads to the closely spaced energy levels becoming discrete states, well separated in energy, suppressing this mechanism. In a real quantum dot, spreading over the available confined states in the mechanism remains responsible for the increase in radiative lifetime.^{7,18,19} The conduction band states in a quantum dot are more widely spaced than the valence band states, owing to the higher effective mass of the holes. Accordingly, the spread of carriers over the available hole states is believed to be the major mechanism for the increase in radiative

lifetime for the quantum dots.^{7,18,19} This is consistent with our results: the increase of the excited state radiative lifetime of the undoped sample is twice that of the doped sample by room temperature, indicating p-doping suppresses the increase of this lifetime.

For a more quantitative discussion, we consider a simple physical model of the QD as a 2D harmonic oscillator,¹⁶ in which the electron (hole) states $e1, e2, e3 \dots (h1, h2, h3)$ are evenly spaced with energy separation $\Delta E_e (\Delta E_h)$. The degeneracies of these levels are 2, 4, 6 (accounting for the spin degeneracy). Under these circumstances, we expect the strong parity-preserving selection rules^{16,20} indicated in Figure 3 for both samples.

Capacitance-voltage spectroscopy of similar QDs under magnetic fields has found an electron spacing ΔE_e of ~ 50 meV (Ref. 16) and a hole spacing ΔE_h between 20 meV and 30 meV.²¹

For the undoped sample, as the temperature increases the holes thermalize across the higher lying energy states $h2$ and $h3$. As the selection rules forbid $e2$ - $h3$ emission, the radiative lifetime of the excited state increases with the occupation of the higher lying energy states, and thus with temperature. (This is the same behavior that has been observed in quantum well (QW)¹⁷ and QD¹⁴ ground states). As the temperature increases, holes can be promoted to the $h3$ level; the parity selection rules forbid $h3$ recombination with an $e2$ electron, which leads to an increase in the radiative lifetime. The activation energy for this process is the separation between the $h1$ and $h3$ levels, which is $2\Delta E_h$, which is between 40 and 60 meV.²² This is consistent with our measured value of 43 ± 5 meV.

For the p-doped sample, hole states are already occupied up to the $h3$ level even at low temperatures, due to the presence of p-doping. Consequently, the $h2$ level will remain occupied at higher temperatures compared with the undoped sample. This explains the slower increase in the radiative lifetime with temperature. However, as the highest temperatures are approached, the excess holes escape from the QD, and the lifetime increases as for the undoped case: the activation energy should, once again, be $2\Delta E_h$ (40–60 meV). This is consistent with our measured value of 36 ± 5 meV.

In conclusion, by use of time-integrated and time-resolved spectroscopy, we have experimentally uncovered the intuitively expected dynamics of the radiative lifetime of the

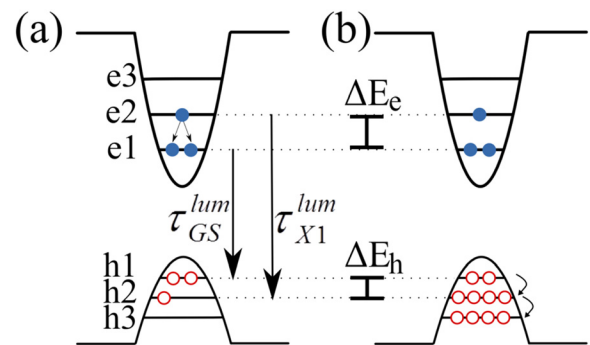


FIG. 3. Schematic of (a) undoped and (b) doped QDs under excitation levels greater than 1 e-h pair per QD. The GS ($e1$ - $h1$) and X1 ($e2$ - $h2$) transitions are marked, and the spacing of the electrons (hole) states is $\Delta E_e (\Delta E_h)$. In the doped sample, the excess holes fill up the valence states.

excited state of quantum dots, and demonstrated that modest amounts of p-doping can suppress the increase of this radiative lifetime with temperature. The low temperature lifetimes are comparable but the lifetime of the undoped sample increased with temperature at twice the rate of the p-doped sample. We attribute this to the presence of holes in the lower confined states at higher temperatures due to the p-doping of the QDs.

This work was supported by Project for Developing Innovation Systems of the Ministry of Education, Culture, Sports, Science and Technology (MEXT), Japan and the Engineering and Physical Sciences Research Council, UK. E.H. gratefully acknowledges support from the Daiwa Anglo-Japanese Foundation, and the Japan Society for the Promotion of Science.

¹Y. Arakawa and H. Sakaki, *Appl. Phys. Lett.* **40**, 939 (1982).

²K. J. Vahala and C. E. Zah, *Appl. Phys. Lett.* **52**, 1945 (1988).

³D. Deppe, H. Huang, and O. B. Shchekin, *IEEE J. Quantum Electron.* **38**(12) 1587–1593 (2002); O. B. Shchekin and D. G. Deppe, *Appl. Phys. Lett.* **80**, 3277 (2002).

⁴A. Markus, J. X. Chen, C. Paranthoën, A. Fiore, C. Platz, and O. Gauthier-Lafaye, *Appl. Phys. Lett.* **82**, 1818 (2003).

⁵P. Spencer, E. M. Clarke, P. Howe, and R. Murray, *Electron. Lett.* **43**, 574 (2007).

⁶S. Raymond, S. Fafard, P. J. Poole, A. Wojs, P. Hawrylak, S. Charbonneau, D. Leonard, R. Leon, P. M. Petroff, and J. L. Merz, *Phys. Rev. B* **54**, 11548–11554 (1996).

⁷H. Yu, S. Lycett, C. Roberts, and R. Murray, *Appl. Phys. Lett.* **69**, 4087 (1996).

⁸K. Mukai, N. Ohtsuka, H. Shoji, and M. Sugawara, *Phys. Rev. B* **54**, R5243–R5246 (1996).

⁹S. Malik, E. C. Le Ru, D. Childs, and R. Murray, *Phys. Rev. B* **63**, 155313 (2001).

¹⁰M. Gurioli, A. Vinattieri, M. Zamfirescu, M. Colocci, S. Sanguinetti, and R. Nötzel, *Phys. Rev. B* **73**, 085302 (2006).

¹¹E. Harbord, P. Spencer, E. Clarke, and R. Murray, *J. Appl. Phys.* **105**, 033507 (2009).

¹²J. Siegert, S. Marcinkevičius, and Q. X. Zhao, *Phys. Rev. B* **72**, 085316 (2005).

¹³D. L. Miller and P. M. Asbeck, *J. Appl. Phys.* **57**, 1816 (1985).

¹⁴E. Harbord, P. Spencer, E. Clarke, and R. Murray, *Phys. Rev. B* **80**, 195312 (2009).

¹⁵D. H. Zhang, K. Radhakrishnan, and S. F. Yoon, *J. Cryst. Growth* **148**, 35–40 (1995).

¹⁶R. J. Warburton, B. T. Miller, C. S. Dürr, C. Bödefeld, K. Karrai, J. P. Kotthaus, G. Medeiros-Ribeiro, P. M. Petroff, and S. Huant, *Phys. Rev. B* **58**, 16221–16231 (1998).

¹⁷R. C. Miller, D. A. Kleinman, W. A. Nordland, Jr., and A. C. Gossard, *Phys. Rev. B* **22**, 863–871 (1980).

¹⁸H. Gotoh, H. Ando, and T. Takagahara, *J. Appl. Phys.* **81**, 1785 (1997).

¹⁹Z. Xu, Y. Zhang, and J. M. Hvan, *Appl. Phys. Lett.* **93**, 183116 (2008).

²⁰I. E. Itskevich, M. S. Skolnick, D. J. Mowbray, I. A. Trojan, S. G. Lyapin, L. R. Wilson, M. J. Steer, M. Hopkinson, L. Eaves, and P. C. Main, *Phys. Rev. B* **60**, R2185 (1999).

²¹D. Reuter, P. Kailuweit, A. D. Wieck, U. Zeitler, O. Wibbelhoff, C. Meier, A. Lorke, and J. C. Maan, *Phys. Rev. Lett.* **94**, 026808 (2005).